

NASA TECHNICAL NOTE



NASA TN D-2921

NASA TN D-2921

N65-28637

FACILITY FORM 502

(ACCESSION NUMBER)
<u>19</u>
(PAGES)
(NASA CR OR TMX OR AD NUMBER)

(THRU)
<u>1</u>
(CODE)
<u>B</u>
(CATEGORY)

GPO PRICE \$ _____
CFST1
OTS PRICE(S) \$ 1.00

Hard copy (HC) _____

Microfiche (MF) .50

IONOSPHERE TOPSIDE SOUNDER STUDIES

II—THE CALCULATION OF THE ELECTRON DENSITY AND THE MAGNETIC FIELD PARAMETERS AT THE ALOUETTE I ORBIT

*by J. O. Thomas, M. J. Rycroft, Margaret Covert,
B. R. Briggs, and L. Colin*

*Ames Research Center
Moffett Field, Calif.*

IONOSPHERE TOPSIDE SOUNDER STUDIES

II - THE CALCULATION OF THE ELECTRON DENSITY AND THE
MAGNETIC FIELD PARAMETERS AT THE ALOUETTE I ORBIT

By J. O. Thomas, M. J. Rycroft, Margaret Covert,
B. R. Briggs, and L. Colin

Ames Research Center
Moffett Field, Calif.

NATIONAL AERONAUTICS AND SPACE ADMINISTRATION

For sale by the Clearinghouse for Federal Scientific and Technical Information
Springfield, Virginia 22151 - Price \$1.00

TABLE OF CONTENTS

	<u>Page</u>
SUMMARY	1
INTRODUCTION	1
PRINCIPLE OF THE METHOD	2
The Determination of the Satellite's Position at a Given Time	3
Computation of Magnetic Field Parameters	5
Output Formats	6
Some Typical Results	7
Inaccuracies in N_V	8
REFERENCES	10
TABLES	11

IONOSPHERE TOPSIDE SOUNDER STUDIES, II: THE CALCULATION
OF THE ELECTRON DENSITY AND THE MAGNETIC FIELD
PARAMETERS AT THE ALOUETTE I ORBIT

By J. O. Thomas, M. J. Rycroft, Margaret Covert,
B. R. Briggs, and L. Colin
Ames Research Center

SUMMARY

28637

In a companion report by Thomas et al., 1965, a number of digital computer programs for reducing Alouette I topside ionograms to electron density profiles were described. These computations can only be carried out accurately if the electron number density and the strength and direction of the earth's magnetic field are known at the vehicle at the time when the ionogram was made. It is the purpose of this report to describe a digital computer program by means of which these quantities can be determined from the Alouette I orbital data and from a measurement of the frequency at which the Extraordinary trace on the ionogram has zero range. The errors involved in the observations and in the calculations are discussed and examples given of some typical results showing the variation of the electron density in the neighborhood of the satellite as a function of time and location.

Author

INTRODUCTION

A measurement of the electron density, N_V , in the vicinity of the Alouette vehicle is important for the physics of the earth's upper atmosphere since the orbit (at circa 1000 km above the surface of the earth) lies at the base of the terrestrial exosphere. The magnitude of the electron density at the vehicle is also an important starting parameter for the calculation of electron density profiles from topside ionograms. These computations require a knowledge of the direction (I_V) and magnitude (B_V) of the earth's field at the Alouette orbit. It is the purpose of this report to describe how the electron density at the vehicle may be calculated from observations of the frequency (f_{XV}) at which the Extraordinary ray has zero range on the topside ionogram and how the magnetic parameters can be derived from Alouette orbital data. A digital computer program for carrying out these computations is described. The errors involved are discussed and figures showing typical results are presented. Programs for computing the electron density profile ($N(h)$ curve) from the observed ionogram using the already computed values of N_V , I_V , and B_V are described in a companion report (ref. 1).

The work described in this report is an extension of that described earlier by Thomas and Sader (refs. 2 and 3). It differs, however, in two important ways: First, more detailed orbital prediction data which have recently become available are now used and, secondly, the magnetic field

parameters are evaluated from the positional and altitude information by means of spherical harmonic expansion coefficients of the earth's field as computed by Jensen and Cain (ref. 4). Both of these factors increase the accuracy of the computations for a given accuracy in the measurement of the observed quantity f_{XV} .

The authors wish to acknowledge gratefully the courtesy of scientists of the Canadian Defence Research Telecommunications Establishment, Ottawa, Canada, particularly Dr. J. H. Chapman and Dr. G. L. Nelms, who made a number of topside ionograms available to the authors in the early stages of development of this work. They wish also to thank the staff of the Radioscience Laboratory, Stanford University, for recording ionograms.

PRINCIPLE OF THE METHOD

Alouette I was launched by NASA on September 29, 1962, into an almost circular orbit around the earth at a height of between approximately 1000 and 1050 km, with an inclination of 80.47° . This polar orbit is such that the satellite is within range of any ground telemetry station at least twice per day. One of the experiments aboard the satellite consists of a topside ionospheric sounder built by the Canadian Defence Research Telecommunications Establishment and is essentially an ionosonde traveling at 26,500 km/hr. Those radio waves from the swept-frequency transmitter which propagate down into the ionosphere are reflected, and an echo is received at the satellite. As the frequency sweeps from 0.45 to 11.8 Mc/s, the time delay between transmitted and echoing pulses is recorded. This information is telemetered to the stations listed in table I, and recorded on magnetic tape. The observational data are then transcribed on to 35-mm photographic film; timing information is simultaneously recorded. A typical ionogram recorded at Stanford University is shown in figure 1. Full details concerning the satellite and its orbit

together with detailed information about the experiments are given in references 2, 3, and 5.

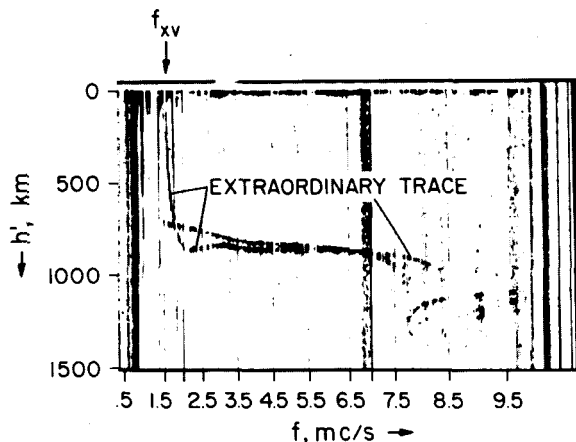


Figure 1.- A daytime topside ionogram recorded at Stanford University.

To calculate the electron density at the vehicle, N_V , the frequency (f_{XV}) at which the Extraordinary trace has zero range (i.e., zero time delay) is measured on the topside ionogram (Lockwood, ref. 6; Thomas and Sader, refs. 2, 3) and the magneto-ionic relationship for "corresponding" frequencies

$$X = 1 - Y \quad (1)$$

first given by Appleton (ref. 7) is used. In this equation, $X = f_N^2/f^2$ and $Y = f_H/f$ where f_N is the plasma frequency, f is the frequency (measured on the Extraordinary ray), and f_H is the gyrofrequency for electrons at the location where the plasma frequency is f_N . Denoting quantities measured at the vehicle by the subscript v , one obtains

$$N_v = \frac{4\pi^2 \epsilon_0 m}{e^2} f_N^2 = 1.2388 \times 10^4 (f_{xv}^2 - f_{xv} f_{Hv}) \quad (2)$$

where e and m , respectively, are the charge and mass of the electron, and ϵ_0 is the permittivity of free space. The frequencies are measured in Mc/s, and N_v is the number of electrons per cubic centimeter at the vehicle. In these equations, f_{Hv} , the electron gyrofrequency at the point of observation, is given by

$$f_{Hv} = \frac{eB_v}{2\pi m} \quad (3)$$

or

$$f_{Hv} = 2.7994 B_v \text{ Mc/s} \quad (4)$$

with B_v , the magnitude of the earth's field at the vehicle, in gauss.

Thus, N_v can be computed from equation (2) using the observed quantity, f_{xv} , provided f_{Hv} is known. The latter can be computed from equation (4) if the magnitude, B_v , of the earth's field at the vehicle is known at the time at which f_{xv} was observed; B_v can be determined from a knowledge of the position of the satellite as described in the next section.

The Determination of the Satellite's Position at a Given Time

The satellite's position at a given time may be determined from details of its orbit, that is, from Alouette positional data, predicted values. The same procedure can be used with the a posteriori orbital data referred to as refined world maps. The satellite's geographic latitude, θ , geographic longitude, Φ , and height are listed at 1-minute intervals (universal time) as shown in table II in degrees to two decimal figures. The height, h , above the international ellipsoid, column 010 H in table II, is given to one decimal figure,¹ the position of the decimal point being known implicitly.

It should be noted that θ is positive to the north and negative to the south, with $|\theta| < 80.47^\circ$, the inclination of the satellite's orbit to the earth's axis; Φ is positive to the east, measured from the Greenwich meridian at $\Phi = +0.00^\circ$, up to $+180.00^\circ$; and Φ is negative to the west, that is, in that direction Φ can lie between -0.00° and -180.00° . There is, therefore, a discontinuity in Φ at the 180° meridian.

¹It should be noted that in refined maps, θ , Φ , and h are given to two more significant figures than they are given in predicted values.

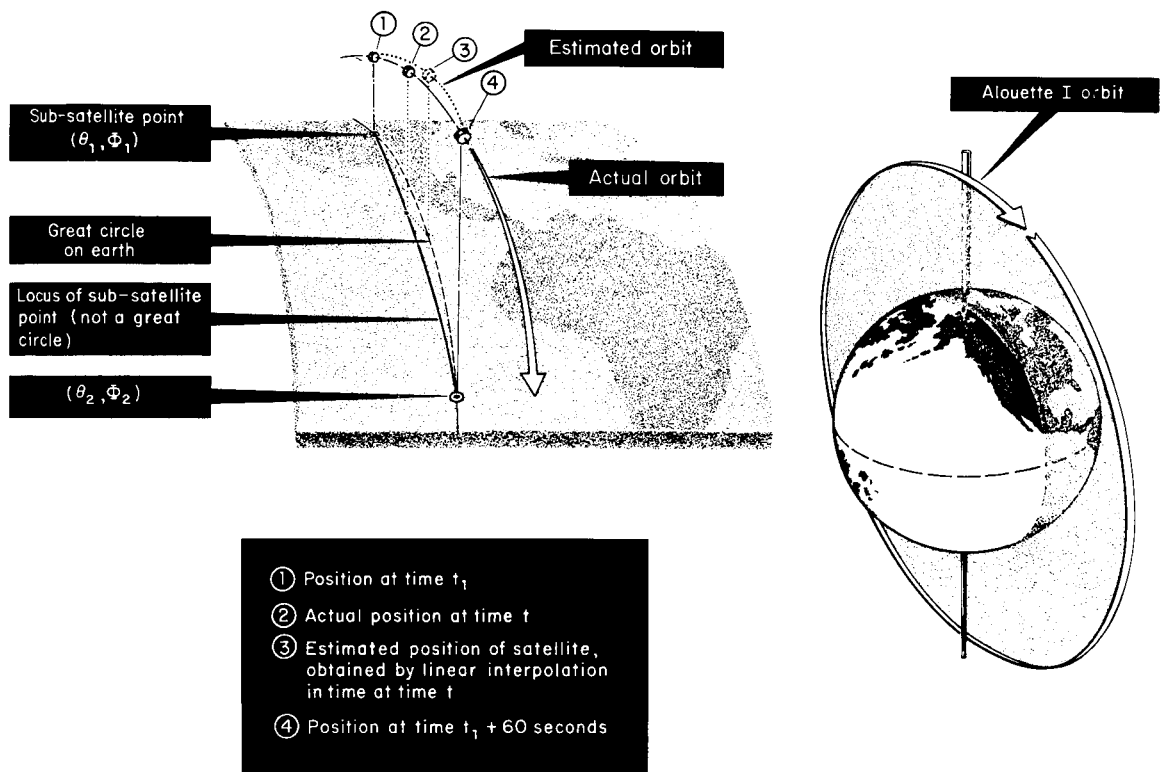


Figure 2.- Diagram showing the difference between the actual and estimated Alouette I orbits (exaggerated); $|\theta_1 - \theta_2|$ is about 3° for positions of the satellite given by world maps at 1-minute intervals.

As indicated in figure 2, a linear interpolation in time between two values 1 minute apart is used to find the values of θ , Φ , and h at the time of the observation of f_{xy} , which is found to ± 0.5 second. At time t , the satellite's latitude is given, to a good approximation at low- and mid-latitudes, by a linear interpolation so that, for example,

$$\theta = \theta_1 + \frac{t - t_1}{60} (\theta_2 - \theta_1) \quad (5)$$

with similar expressions for longitude, Φ , and height, h . The subscripts 1 and 2 denote the values of θ , Φ , or h given just before and just after the time t at which f_{xy} was observed.

Signs are automatically cared for in these equations in all possible cases except near $\Phi = \pm 180^\circ$. If Φ_2 is negative and Φ_1 is positive, Φ_2' should be put equal to $360.00^\circ + \Phi_2$. Then

$$\Phi' = \Phi_1 + \frac{t - t_1}{60} (\Phi_2' - \Phi_1) \quad (6)$$

is calculated. For $\Phi' \leq 180.00^\circ$, the desired Φ is equal to Φ' . For $\Phi' > 180.00^\circ$, the desired Φ equals $-360.00^\circ + \Phi'$.

A set of N cards containing positional data for a certain pass and date is followed by ionogram data cards containing the observations of f_{xy} taken at a certain station for the same pass and date. The card format shown in the lower part of table III is used for the ionogram data, and is similar to that used for the positional data. The ionogram data cover a time range of $(N - 1)$ minutes, typically 10 minutes. All observations thus lie within the range of times given in the positional input data. Up to $60(N - 1)/18$ readings of f_{xy} are possible, since the frame repetition period is 18 seconds. A typical set of input data is reproduced in table IV.

Computation of Magnetic Field Parameters

The values of θ , Φ , and h computed using equation (5) locate the point in space at which the observation was made. Given these three quantities, a computer program furnished by NASA Goddard Space Flight Center calculates the magnitude B_v of the magnetic field at that point from its three components. The program uses coefficients for a 48-term expansion in spherical harmonics of the earth's field (ref. 4).

The predicted value data are punched on to computer input cards in the format shown in table III. Additional information read into the machine and printed on the standard output formats include:

(1) The three-hourly K_p index of magnetic activity (columns 46 and 47, table III)

(2) An asterisk if the satellite is in sunlight (column 41, table III). The asterisk appears to the right of the height column in table II.

(3) Magnetic coordinates L , λ_{dip} , and A_{inv} ht computed as described below.

McIlwain's (ref. 8) parameter L is defined so that

$$\left(\frac{L^3 B}{M}\right)_{\text{actual field}} = \left(\frac{R_{eq}^3 B}{M}\right)_{\text{pure dipole field}} \quad (7)$$

For the actual geomagnetic field, L is the analog of R_{eq} , the distance in earth radii to a line of force in the equatorial plane for a dipole representation of the earth's magnetic field, of moment M , with M given by

$$M = 8.06 \times 10^{25} \text{ gauss cm}^3 = (0.311653 \text{ gauss}) R_E^3 \quad (8)$$

in which R_E is the radius of the earth (approximated as a sphere) and is taken to be 6371.2 km. In this definition, the effects of nondipole terms are included, whereas those of external current systems, for example at the magnetospheric boundary, are excluded. The quantity L is computed by integrating a magnetic invariant of the charged particles' motion along the field line from the point of observation to the magnetically conjugate point (E. G. Stassinopoulos, private communication, 1964). A particular line of

force about which and along which the electrons and ions are constrained to move is specified by a particular value of L .

The dip latitude, λ_{dip} , is also computed as follows. From the three field components at the observational point, the dip angle, I_V , the angle that the field line through the point makes with the horizontal, is computed. (The dip angle associated with a particular ionogram is used in the computation of that electron density profile (ref. 1).) By analogy with a dipole field, the dip latitude (Chapman, ref. 9) is defined as

$$\lambda_{\text{dip}} = \arctan\left(\frac{1}{2} \tan I_V\right) \quad (9)$$

It is computed in degrees to two decimal figures.

O'Brien (ref. 10) introduced the invariant geomagnetic latitude, Λ , of a point at the earth's surface for the observed geomagnetic field (but by analogy with a dipole field) as

$$L \cos^2 \Lambda = 1 \quad (10)$$

or

$$\Lambda = \arccos \frac{1}{\sqrt{L}} \quad (11)$$

For any height, h , above the earth's surface this relation may be generalized, defining the invariant geomagnetic latitude at that height, $\Lambda_{\text{inv ht}}$, by

$$L \cos^2 \Lambda_{\text{inv ht}} = \frac{6371.2 + h}{6371.2} \quad (12)$$

h being in km. This quantity is a magnetic latitude which pertains to the entire line of force through the observational point, whereas the dip latitude depends only on the local value of the dip angle. As may be seen from table V, these two latitudes differ by typically 2° at mid-latitudes, with greater differences occurring at dip latitudes above 60° .

Output Formats

The computer output of the N_V program is stored on magnetic tape. An example of the standard output print-out format, for the input data given in table IV, is presented in table V. Each row in this table refers to one ionogram, from which one value of N_V is derived. The various magnetic coordinates discussed previously are also listed.

In order to study the influence of the sun on N_V , the local time corresponding to the universal time and geographic longitude of the point of observation is calculated. The local mean time, in hours and fractions thereof, is calculated from

$$\text{LMT} = (\text{universal time}) + \frac{\Phi}{15} \quad (13)$$

for Φ positive or negative. If this is greater than 24 hours, 24 hours is subtracted to give the local time; the local date is then the universal date +1. If this calculated LMT value is negative, 24 hours is subtracted to give the local time; the local date is then the universal date -1. The local date is printed also.

Some Typical Results

Interesting features of the topside of the ionosphere are evident from studies of N_V alone, even when the complete electron density profile is unknown. Examples of such features are now considered briefly.

The summertime diurnal variation of N_V , computed from ionograms telemetered to Stanford, is presented in figure 3. This figure shows the kinds of variations in N_V that are found; N_V is dependent on local time, magnetic latitude, geographic longitude, height, solar activity, and magnetic K_p index. It is important to note that the standard deviation of a mean value of

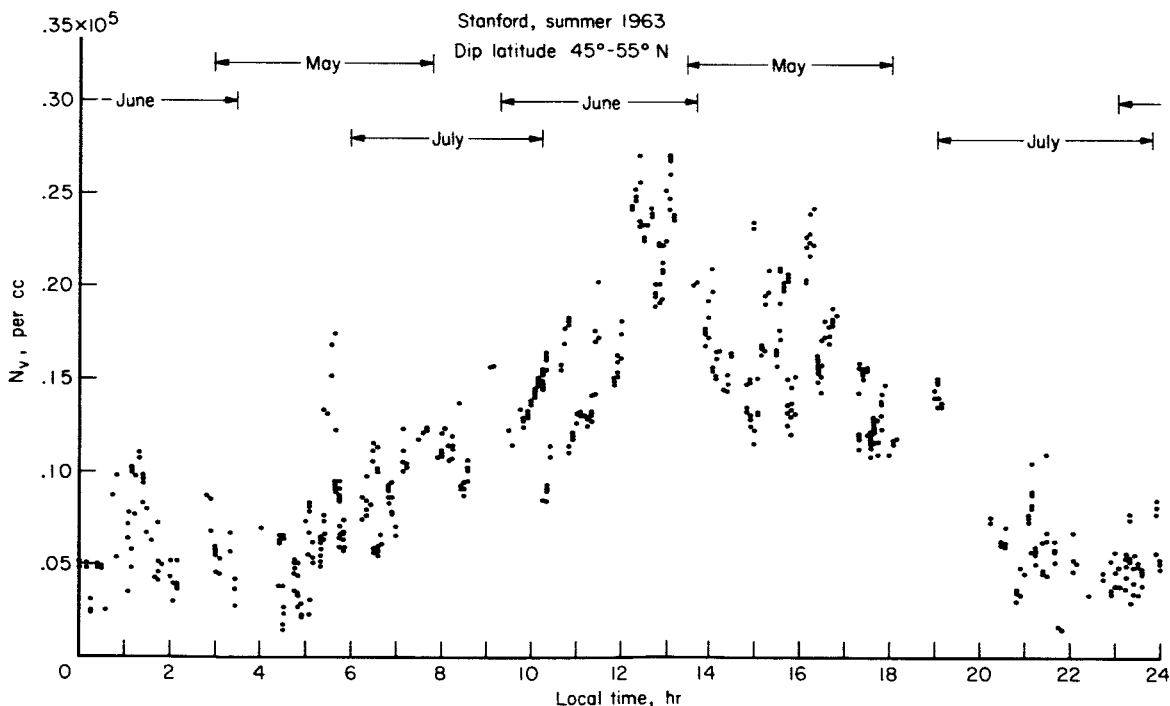


Figure 3.- Diurnal variation of the electron density, N_V , at the Alouette I orbit.

N_V is typically $\pm 0.04 \times 10^5$ per cc, or approximately ± 30 percent. In the following section it is shown that the scatter of the points is authentic and occurs in the ionosphere.

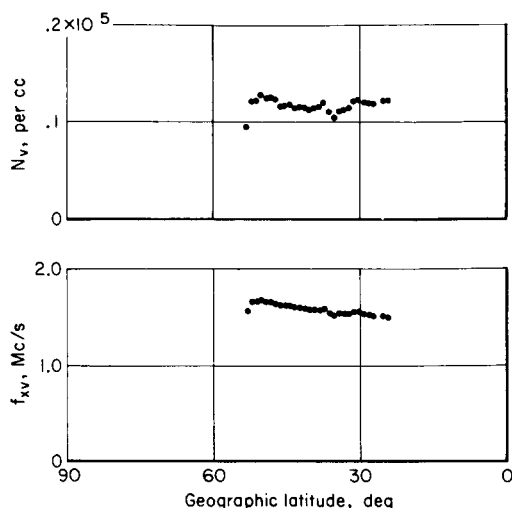


Figure 4.- Automatic plot of f_{XV} and N_V against geographic latitude, calculated from ionograms telemetered to Ottawa on November 10, 1962, pass number 582, $K_p = 2$ - .

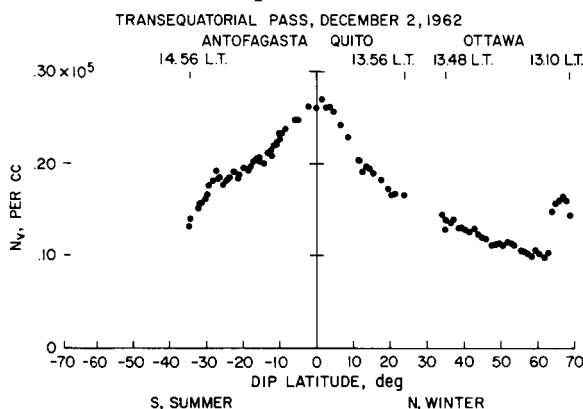


Figure 5.- Variation with dip latitude of the electron density at the Alouette I orbit at a certain local time calculated from ionograms telemetered to three stations on December 2, 1962, pass number 881, $K_p = 1$ + .

An automatic plotter is programmed to plot, on option, N_V against any of the several types of latitude or longitude. Figure 4 is a typical graph of both f_{XV} and N_V versus geographic latitude for the pass considered earlier. A graph of N_V versus dip latitude for ionograms telemetered to three stations during a single pass of the satellite is presented in figure 5. The daytime monotonic decrease of N_V with increasing latitude is apparent from this figure. At dip latitudes greater than 60° , its variation is often complicated.

Inaccuracies in N_V

It is the purpose of this section to consider inherent errors in the computation of N_V and to estimate their magnitudes.

The time associated with a particular frequency marker on an ionogram is recorded to ± 0.5 sec on the film. From this, if a 1 Mc/s^2 sweep rate is assumed, the time at which a particular f_{XV} was observed can be found. Since the satellite moves at about 7 km/sec along its orbit, this corresponds to an inaccuracy of $\pm 3.5 \text{ km}$ in horizontal position for the measurement. For maximum accuracy, it is crucial that errors introduced in the computer pro-

gram are not significantly greater than this error; the program was designed with this criterion in mind.

First, it should be noted that, for computing the satellite's position, predicted rather than refined value orbital details are used. The discrepancy between these two values is typically $\pm 3 \text{ km}$, and is thus not important here. It is assumed that neither the predicted value nor the refined value satellite position differs systematically from the true position, nor that there is any significant error in the time of the ionogram as recorded on the film.

Second, in order to find the satellite's position at any instant, a linear interpolation in time is used between geographic latitude and longitude

coordinates given at 1-minute intervals. As the satellite moves northward from the equator, typical differences in latitude and longitude between these 1-minute intervals are given in table VI. It is evident from the manner in which these differences change with latitude that a linear interpolation in time will lead to greater errors at higher latitudes. The linear interpolation in latitude leads to an error in latitudinal position of less than ± 10 km for geographic latitudes up to 65° , whereas that in longitude leads to an error in longitudinal position of less than ± 10 km for geographic latitudes up to 40° . An error in position of ± 10 km is reflected as an error in the magnetic field at the observational point of less than ± 0.1 percent, thus, f_{Hv} is typically in error by ± 0.001 Mc/s. Differentiating equation (2) shows that this causes a negligible error in N_v of only ± 0.1 percent, or 20 per cc, for typical mid-latitude daytime conditions.

For latitudes between 40° and 65° , the error in longitudinal position is greater than ± 10 km. However, this is not reflected as a serious error in f_{Hv} because lines of constant total magnetic field intensity are nearly parallel to parallels of latitude. At latitudes near 75° , the positional inaccuracy could become more than 100 km, with an associated error in B_v of up to ± 0.01 gauss, or in the computed N_v , of up to $\pm 0.001 \times 10^5$ per cc.

Hence, the interpolations used in finding the value of the magnetic field are entirely adequate at all latitudes concerned, for the determination of N_v to considerably better than $\pm 0.01 \times 10^5$ per cc.

The accuracy to which f_{xv} may be read is now considered. Recourse to figure 1 shows the width of the Extraordinary trace near f_{xv} to be typically 0.05 Mc/s; a strong case can be made for reading f_{xv} at the center of the trace. The frequency is found by linear interpolation between the frequency markers on either side of the trace, usually the 0.5 and 1.5 Mc/s, or 1.5 and 2.0 Mc/s, markers.

The film is conveniently read when an enlarged image of each ionogram is projected and a digitizer is used which produces the $h'(f)$ data on punched cards. The typical error in setting the digitizer on the frequency f_{xv} and the nearest frequency markers on each side of f_{xv} is 0.02 Mc/s, causing a typical error of $\pm \sqrt{3(0.02)^2} \approx \pm 0.035$ Mc/s in f_{xv} . The effect of this error on the computed N_v is shown in table VII for typical day and night conditions above various stations (having different values of the gyrofrequency at 1000 km). The electron density at the Alouette I orbit is thus found to an accuracy of approximately $\pm 0.01 \times 10^5$ per cc, effectively determined by the accuracy to which f_{xv} may be read, so that the standard deviation of the points in figure 3 ($\pm 0.04 \times 10^5$ per cc) is due mainly to variations in the ionosphere.

Ames Research Center
National Aeronautics and Space Administration
Moffett Field, Calif., Mar. 2, 1965

REFERENCES

1. Thomas, J. O., Briggs, B. R., Colin, L., Rycroft, M. J., and Covert, Margaret: Ionosphere Topside Sounder Studies, I: The Reduction of Alouette I Ionograms to Electron Density Profiles. NASA TN D-2882, 1965.
2. Thomas, J. O., and Sader, A. Y.: Alouette Topside Soundings Monitored at Stanford University. Tech. Rep. 6, NASA Grant NsG 30-60, Stanford Electronics Lab., Stanford University, 1963.
3. Thomas, J. O., and Sader, A. Y.: Electron Density at the Alouette Orbit. J. Geophys. Res., vol. 69, no. 21, Nov. 1964, pp. 4561-81.
4. Jensen, D. C., and Cain, J. C.: An Interim Geomagnetic Field. J. Geophys. Res., vol. 67, no. 9, August 1962, p. 3568.
5. Canadian Defence Research Telecommunications Establishment: Alouette, Satellite 1962 Beta Alpha One. Canadian Defence Research Board, Ottawa, Canada, 1962.
6. Lockwood, G. E. K.: Plasma and Cyclotron Spike Phenomena Observed in Top-Side Ionograms. Can. J. Phys., vol. 41, no. 1, Jan. 1963, pp. 190-4.
7. Appleton, E. V.: Wireless Studies of the Ionosphere. J. Inst. Elec. Engr., vol. 71, 1932, p. 642.
8. McIlwain, Carl E.: Coordinates for Mapping the Distribution of Magnetically Trapped Particles. J. Geophys. Res., vol. 66, no. 11, Nov. 1961, pp. 3681-91.
9. Chapman, Sydney: Geomagnetic Nomenclature. J. Geophys. Res., vol. 68, no. 4, Feb. 1963, p. 1174.
10. O'Brien, B. J.: A Large Diurnal Variation of the Geomagnetically Trapped Radiation. J. Geophys. Res., vol. 68, no. 4, Feb. 1963, pp. 989-95.

TABLE I.- TOPSIDE SOUNDER TELEMETRY STATIONS

Station location	Geographic latitude	Geographic longitude	NASA code	Gyrofrequency at 1000 km from B, L map, Mc/s
Antofagasta, Chile	-23.62	-70.27	AGASTA	0.501
Blossom Point, Maryland	+38.43	-77.07	BPOINT	.982
Boulder, Colorado	+40.01	-105.25	BOULDR	.994
College, Alaska	+64.87	-147.80	COLERGE	1.038
E. Grand Forks, Minnesota	+47.95	-97.08	GFORKS	1.055
Fort Myers, Florida	+26.55	-81.87	FTMYRS	.879
Hawaiian Islands (South Point)	+18.93	+155.68	SPOINT	.644
Ottawa, Canada	+45.40	-75.72	1HWPMP	1.027
Prince Albert, Canada	+53.22	-105.93	1OTTWA	1.066
Quito, Ecuador	-00.62	-78.58	2PRINC	.588
Resolute Bay, Canada	+74.67	-95.00	QUITOE	1.08
St. Johns, Canada	+45.57	-52.41	1RSLUT	.971
Santiago, Chile	-50.46	-75.26	NEWFLD	.532
Singapore, Malaya	+01.32	+103.82	SNTAGO	.722
South Atlantic (Falkland Is.)	-51.75	-57.93	SNGPOR	.641
Stanford, California	+37.43	-122.16	SATLAN	.854
Winkfield, England	+51.45	-00.42	STNFRD	.882
Woomera, Australia	-31.10	-136.78	WNKFLD	.764
			OOMERA	

NOTE: + = North, - = South for latitude
+ = East, - = West for longitude

TABLE II.- ALOUETTE POSITIONAL DATA - PREDICTED VALUES

S 27 WORLD MAP

PASS NO. 00582 OF SATELLITE 62491 . DATE 621110
 205822 119.88 00.00 010304*

DATE 621110

TIME	LONG.	LAT.	010 H.	TIME	LONG.	LAT.	010 H.
HRMISE	DEG.	DEG.	KM.	HRMISE	DEG.	DEG.	KM.
205900	120.02	02.11	010305*	213700	-080.46	47.70	010226*
210000	120.34	05.48	010307*	213800	-079.54	44.39	010215*
210100	120.66	08.86	010310*	213900	-078.75	41.06	010204*
210200	121.00	12.24	010315*	214000	-078.06	37.72	010192*
210300	121.34	15.61	010320*	214100	-077.44	34.37	010179*
210400	121.71	18.98	010326*	214200	-076.90	31.02	010166*
210500	122.10	22.34	010332*	214300	-076.41	27.65	010153*
210600	122.53	25.69	010340*	214400	-075.96	24.28	010140*
210700	122.99	29.05	010347*	214500	-075.54	20.90	010128*
210800	123.50	32.39	010354*	214600	-075.16	17.52	010117*
210900	124.06	35.73	010362*	214700	-074.80	14.13	010106*
211000	124.70	39.06	010370*	214800	-074.45	10.74	010098*
211100	125.43	42.38	010377*	214900	-074.12	07.34	010091*
211200	126.26	45.69	010385*	215000	-073.80	03.95	010085*
211300	127.24	48.99	010392*	215100	-073.48	00.55	010082*
211400	128.38	52.27	010399*	215200	-073.17	-02.83	010080*
211500	129.75	55.54	010405*	215300	-072.85	-06.23	010081*
211600	131.41	58.77	010410*	215400	-072.52	-09.62	010083*
211700	133.46	61.98	010414*	215500	-072.18	-13.01	010087*
211800	136.04	65.13	010416*	215600	-071.83	-16.40	010098*
211900	139.38	68.22	010416*	215700	-071.45	-19.79	010100*
212000	143.82	71.20	010414*	215800	-071.05	-23.18	010109*
212100	149.89	74.03	010410*	215900	-070.61	-26.55	010119*
212200	158.44	76.59	010404*	220000	-070.13	-29.93	010130*
212300	170.60	78.72	010396*	220100	-069.60	-33.29	010142*
212400	-172.73	80.12	010387*	220200	-069.01	-36.65	010154*
212500	-152.88	80.48	010376*	220300	-068.34	-40.00	010167*
212600	-133.90	79.69	010363*	220400	-067.58	-43.33	010180*
212700	-119.01	77.96	010350*	220500	-066.71	-46.65	010192*
212800	-108.40	75.64	010336*	220600	-065.69	-49.96	010203*

TABLE III.- INPUT FOR N_v PROGRAM

FORMAT (I6,2(I3,I2,I2),F7.2,F6.2,F7.1,A1,A6)

X = DECIMAL DATA

B = BLANK

A = HOLLERITH INFORMATION

* = SUNLIGHT INDICATOR, * OR B

DATA IS RIGHT JUSTIFIED IN ITS FIELD

POSITIONAL DATA

PASS	DATE YRMODY	TIME HRMNSC	LONG	LAT	OIO H	*	KP
123456	1111 7890123	1111112 4567890	2222222 1234567	223333 890123	3333334 4567890	4 1	4444444 234567
XXXXXX	XXXXXX	XXXXXX	±XXX.XX	±XX.XX	BOXXXXX	A	BBBBAA

IONOGRAM DATA

PASS	DATE YRMODY	TIME HRMNSC	FXV		STATION
123456	1111 7890123	1111112 4567890	2222222 1234567	22333333333344 89012345678901	4444444 234567
XXXXXX	XXXXXX	XXXXXX	X.XX	BBBBBBBBBBBBBB	AAAAAA

TABLE IV.- INPUT DATA FOR PASS NUMBER 582, DATE 621110

Positional data	000582	621110	213500-082.81	54.27	010247*	2-
	000582	621110	213600-081.53	51.00	010237*	2-
	000582	621110	213700-080.46	47.70	010226*	2-
	000582	621110	213800-079.54	44.39	010215*	2-
	000582	621110	213900-078.75	41.06	010204*	2-
	000582	621110	214000-078.06	37.72	010192*	2-
	000582	621110	214100-077.44	34.37	010179*	2-
	000582	621110	214200-076.90	31.02	010166*	2-
	000582	621110	214300-076.41	27.65	010153*	2-
	000582	621110	214400-075.96	24.28	010140*	2-
Ionogram data	000582	621110	213512	1.55		OTTAWA
	000582	621110	213530	1.65		OTTAWA
	000582	621110	213548	1.65		OTTAWA
	000582	621110	213606	1.67		OTTAWA
	000582	621110	213624	1.65		OTTAWA
	000582	621110	213642	1.65		OTTAWA
	000582	621110	213700	1.64		OTTAWA
	000582	621110	213718	1.61		OTTAWA
	000582	621110	213736	1.61		OTTAWA
	000582	621110	213754	1.61		OTTAWA
	000582	621110	213812	1.59		OTTAWA
	000582	621110	213831	1.59		OTTAWA
	000582	621110	213849	1.58		OTTAWA
	000582	621110	213907	1.57		OTTAWA
	000582	621110	213925	1.57		OTTAWA
	000582	621110	213943	1.57		OTTAWA
	000582	621110	214001	1.58		OTTAWA
	000582	621110	214019	1.54		OTTAWA
	000582	621110	214037	1.51		OTTAWA
	000582	621110	214055	1.53		OTTAWA
	000582	621110	214113	1.53		OTTAWA
	000582	621110	214132	1.53		OTTAWA
	000582	621110	214150	1.55		OTTAWA
	000582	621110	214208	1.55		OTTAWA
	000582	621110	214226	1.53		OTTAWA
	000582	621110	214244	1.52		OTTAWA
	000582	621110	214302	1.51		OTTAWA
	000582	621110	214338	1.51		OTTAWA
	000582	621110	214356	1.50		OTTAWA

TABLE V.- ALOUETTE TOPSIDE SOUNDER OBSERVATIONS AT OTTAWA PASS NUMBER 582

UNIVERSAL			LOCAL			SNL	LONG	LAT	HEIGHT	FXV	FHV	H	DIP ANGLE	LAMBDA DIP	LAMBDA IHVHT	L	N 10-5	KP
DATE YRWDY	TIME HRMNSC	MO	TIME HRMNSC	DY	NOV.													
621110	213512	10	NOV.	16	459	*	-82.55	53.62	1024.5	1.55	1.06	0.3780	79.29	69.28	65.66	6.834	0.094	2-
621110	213530	10	NOV.	16	649	*	-82.17	52.63	1024.2	1.65	1.05	0.3769	78.73	68.28	64.74	6.376	0.122	2-
621110	213548	10	NOV.	16	839	*	-81.79	51.65	1023.9	1.65	1.05	0.3756	78.16	67.26	63.82	5.963	0.122	2-
621110	2136 6	10	NOV.	16	1024	*	-81.42	50.67	1023.6	1.67	1.05	0.3743	77.58	66.23	62.89	5.591	0.129	2-
621110	213624	10	NOV.	16	1159	*	-81.10	49.68	1023.3	1.65	1.04	0.3728	76.99	65.19	61.96	5.251	0.124	2-
621110	213642	10	NOV.	16	1334	*	-80.78	48.69	1022.9	1.65	1.04	0.3713	76.38	64.15	61.02	4.944	0.125	2-
621110	2137 0	10	NOV.	16	15 9	*	-80.46	47.70	1022.6	1.64	1.03	0.3696	75.76	63.09	60.08	4.664	0.123	2-
621110	213718	10	NOV.	16	1633	*	-80.18	46.71	1022.3	1.61	1.03	0.3678	75.13	62.03	59.13	4.409	0.116	2-
621110	213736	10	NOV.	16	1758	*	-79.91	45.71	1021.9	1.61	1.02	0.3660	74.49	60.96	58.19	4.175	0.117	2-
621110	213754	10	NOV.	16	1922	*	-79.63	44.72	1021.6	1.61	1.02	0.3640	73.83	59.89	57.24	3.963	0.118	2-
621110	213812	10	NOV.	16	2040	*	-79.38	43.72	1021.3	1.59	1.01	0.3618	73.16	58.81	56.29	3.766	0.114	2-
621110	213831	10	NOV.	16	2159	*	-79.13	42.67	1020.9	1.59	1.01	0.3595	72.44	57.67	55.27	3.575	0.115	2-
621110	213849	10	NOV.	16	2314	*	-78.89	41.67	1020.6	1.58	1.00	0.3571	71.74	56.58	54.32	3.410	0.114	2-
621110	2139 7	10	NOV.	16	2426	*	-78.67	40.67	1020.3	1.57	0.99	0.3547	71.03	55.49	53.36	3.257	0.112	2-
621110	213925	10	NOV.	16	2534	*	-78.46	39.67	1019.9	1.57	0.99	0.3521	70.30	54.39	52.39	3.115	0.114	2-
621110	213943	10	NOV.	16	2641	*	-78.26	38.67	1019.5	1.57	0.98	0.3495	69.56	53.30	51.43	2.985	0.115	2-
621110	2140 1	10	NOV.	16	2749	*	-78.05	37.66	1019.2	1.58	0.97	0.3467	68.80	52.20	50.47	2.863	0.119	2-
621110	214019	10	NOV.	16	2851	*	-77.86	36.66	1018.8	1.54	0.96	0.3438	68.03	51.10	49.49	2.749	0.110	2-
621110	214037	10	NOV.	16	2954	*	-77.68	35.65	1018.4	1.51	0.95	0.3409	67.24	50.00	48.53	2.645	0.104	2-
621110	214055	10	NOV.	16	3057	*	-77.49	34.65	1018.0	1.53	0.95	0.3378	66.44	48.90	47.56	2.547	0.111	2-
621110	214113	10	NOV.	16	3155	*	-77.32	33.64	1017.6	1.53	0.94	0.3346	65.61	47.80	46.60	2.456	0.112	2-
621110	214132	10	NOV.	16	3255	*	-77.15	32.58	1017.2	1.53	0.93	0.3312	64.73	46.65	45.58	2.367	0.114	2-
621110	214150	10	NOV.	16	3352	*	-76.99	31.58	1016.8	1.55	0.92	0.3279	63.87	45.55	44.61	2.288	0.121	2-
621110	2142 8	10	NOV.	16	3447	*	-76.83	30.57	1016.4	1.55	0.91	0.3245	63.00	44.45	43.65	2.214	0.123	2-
621110	214226	10	NOV.	16	3540	*	-76.69	29.56	1016.0	1.53	0.90	0.3210	62.10	43.36	42.67	2.145	0.120	2-
621110	214244	10	NOV.	16	3634	*	-76.54	28.55	1015.6	1.52	0.89	0.3174	61.18	42.26	41.71	2.080	0.119	2-
621110	2143 2	10	NOV.	16	3727	*	-76.39	27.54	1015.3	1.51	0.88	0.3137	60.24	41.17	40.74	2.019	0.118	2-
621110	214338	10	NOV.	16	39 8	*	-76.12	25.52	1014.5	1.51	0.86	0.3062	58.30	38.99	38.82	1.909	0.122	2-
621110	214356	10	NOV.	16	3958	*	-75.99	24.50	1014.1	1.50	0.85	0.3024	57.30	37.91	37.85	1.859	0.121	2-

TABLE VI.- GEOGRAPHIC LATITUDE AND LONGITUDE DIFFERENCES BETWEEN VALUES AT ONE-MINUTE INTERVALS FOR A NORTHWARD PASS OF ALOUETTE I (NASA PREDICTED VALUES)

Geographic latitude, N, deg	Latitude difference, deg	Longitude difference, deg
5	3.40	0.32
15	3.39	.35
25	3.37	.46
35	3.35	.64
45	3.31	.96
55	3.24	1.6
65	3.09	3.1
75	2.2	15

TABLE VII.- ERRORS IN N_V CAUSED BY AN ERROR OF ± 0.035 Mc/s IN f_{XV} FOR VARIOUS VALUES OF f_{XV} AND f_{HV} (THOMAS AND SADER, REF. 2)

f_{HV} , Mc/s	Nighttime, $N_V = 0.05 \times 10^5$ per cc		Daytime, $N_V = 0.20 \times 10^5$ per cc	
	f_{XV} , Mc/s	$\Delta N_V / N_V$, percent	f_{XV} , Mc/s	$\Delta N_V / N_V$, percent
0.6	1.00	12.1	1.60	5.6
.9	1.23	13.4	1.80	5.8
1.2	1.47	15.0	2.00	6.0